Biofilm 7 (2024) 100181

Contents lists available at ScienceDirect

Biofilm

journal homepage: www.sciencedirect.com/journal/biofilm

Bioenergetics of simultaneous oxygen and nitrate respiration and nitric oxide production in a *Pseudomonas aeruginosa* agar colony biofilm

Paul Stoodley [a,b,*], Nina Toelke [c], Carsten Schwermer [d], Dirk de Beer [c]

[a] National Centre for Advanced Tribology at Southampton, (NCATS), Mechanical Engineering, University of Southampton, Southampton, SO17 1BJ, UK
[b] Department of Microbial Infection and Immunity, Department of Orthopaedics, The Ohio State University, 716 Biomedical Research Tower (BRT), 460 W 12th Ave, Columbus OH, 43210, United States
[c] Max Planck Institute for Marine Microbiology (MPI), Microsensor Group and Molecular Ecology Group, Celsiusstrasse 1, D-28359, Bremen, Germany
[d] Norwegian Institute for Water Research (NIVA), Gaustadalléen 21, NO-0349, Oslo, Norway

A B S T R A C T

Pseudomonas aeruginosa is a biofilm forming pathogen commonly associated with infection of the cystic fibrosis (CF) lung, chronic wounds and indwelling medical devices. *P. aeruginosa* is a facultative aerobe that can use nitrate (NO_3^-) found in healthy and infected tissues and body fluids to generate energy through denitrification. Further, *P. aeruginosa* the expression of denitrification genes has been found in specimens from people with CF. The main aim of this study was to determine the relative energy contribution of oxygen (O_2) respiration and denitrification in single *Pseudomonas aeruginosa* PAO1 biofilm colonies under different O_2 concentrations to estimate the possible relative importance of these metabolic processes in the context of biofilm infections. We showed that the used strain PAO1 in biofilms denitrified with nitrous oxide (N_2O), and not nitrogen (N_2), as the end product in our incubations. From simultaneous O_2 and N_2O microprofiles measured with high spatial resolution by microsensors in agar colony biofilms under air, N_2 and pure O_2, the rates of aerobic respiration and denitrification were calculated and converted to ATP production rates. Denitrification occurred both in the oxic and anoxic zones, and became increasingly dominant with decreasing O_2 concentrations. At O_2 concentrations characteristic for tissues and wounds (20–60 μM), denitrification was responsible for 50% of the total energy conservation in the biofilm. In addition the formation of nitric oxide (NO), a precursor of N_2O and an important regulator of many cellular processes, was strongly influenced by the local O_2 concentrations. NO production was inhibited under pure O_2, present under anoxia (~1 μM) and remarkably high (up to 6 μM) under intermediate O_2 levels, which can be found in infected tissues. Possible impacts of such NO levels on both the host and the biofilm bacteria are discussed.

1. Introduction

Pseudomonas aeruginosa is a Gram-negative opportunistic pathogen and is a well characterized biofilm-former responsible for a number of chronic infections [1,2]. Although originally considered generally an aerobic organism, *P. aeruginosa* is also cap(NO_3^-) as an alternative electron acceptor for growth. In an oxic environment *P. aeruginosa* generates strong oxygen (O_2) gradients by rapid consumption of this, energetically most favorable electron acceptor, and the deeper parts of the biofilms can become anoxic[3]. Since NO_3^- is much more soluble in water than O_2 its higher concentrations and lower respiration rates allows deeper penetration into the biofilm than O_2. This allows metabolic activity deeper in the biofilm independent of O_2, thus denitrification may be an important factor in chronic biofilm infections by this pathogen. Both electron acceptors (O_2 and NO_3^-) are present in tissues and fluids in wounds [4] and the diseased lung, as might be found in people with cystic fibrosis [5], which are also commonly infected with *P. aeruginosa*. Further, the expression of *P. aeruginosa* denitrification genes in CF isolates and sputum recovered from chronically infected patients suggesting that denitrification was occurring *in vivo* and might be relevant in the pathogenesis [6,7]. Previously it was shown that O_2 respiration and denitrification could occur at the same depth in a *P. aeruginosa* agar colony biofilm [8]. The aim of the present study was to determine the relative contribution of simultaneous oxygen respiration and denitrification in single *Pseudomonas aeruginosa* agar biofilm colonies under different O_2 concentrations to estimate the possible relative importance of these metabolic processes in the context of biofilm infections. We investigated their relative importance for growth under different levels of O_2 saturation ranging from hypoxic to hyperoxic by switching headspaces gasses (air, pure O_2 and pure nitrogen (N_2)). Due to aerobic respiration, mass transfer resistance, and limited O_2 solubility, anaerobic micro-niches develop in biofilms [9]. Furthermore, in environments where O_2 levels can rapidly change between anoxia and air saturation, denitrification was reported to be insensitive to O_2 [10].

* Corresponding author. National Centre for Advanced Tribology at Southampton, (NCATS), Mechanical Engineering, University of Southampton, Southampton, SO17 1BJ, UK.
E-mail address: P.stoodley@soton.ac.uk (P. Stoodley).

https://doi.org/10.1016/j.biofilm.2024.100181
Received 24 August 2023; Received in revised form 9 January 2024; Accepted 1 February 2024
Available online 10 February 2024

Therefore, we also investigated whether *P. aeruginosa* PAO1 agar colony biofilms were equally insensitive to O_2, and the dynamics of switching between aerobic respiration and denitrification. We used an *in vitro* model to simulate biofilms growing on soft surfaces where colonies of *P. aeruginosa* PAO1 strains grown on agar plates were submerged within a growth medium [8]. Here, we report the changes in local fluxes of O_2 and NO_3^- (from stoichiometry from nitrous oxide (N_2O) measurements) into the colonies under different O_2 concentrations and determined the consequences for bioenergetics. Since an infecting biofilm may be exposed to varying O_2 regimes, we hypothesized that denitrification contributes to energy conservation at varying O_2 levels. Secondly, we expect that due to well adapted e-transfer NO remains low (1 nM), independently from the O_2 supply. Bioenergetic calculations for denitrifying communities were based on data from Strous [11] to estimate the stoichiometry of ATP formed per rate of electron flow with O_2 and NO_3^- as e-acceptor, respectively. Although PAO1 can perform aerobic denitrification we expected effects of local O_2 concentrations on the electron flow to NO_3^- and thus on the denitrification pathway. The effect of different O_2 concentrations on the denitrification intermediate NO was determined by a NO microsensor.

2. Materials and methods

2.1. Bacterial strains, growth conditions and experimental set-up

Details on the growth conditions, the measurement set-up, and the microelectrodes used can be found elsewhere [8]. Briefly, frozen stocks of *P. aeruginosa* PAO1 were streaked onto brain heart infusion (BHI Difco 241,830) and incubated for 24 h at 37 °C. The plates were then transferred to a square glass sided (14 × 14 × 7 cm in dimensions) aquarium reservoir which was gently filled with 0.75 L of minimal salts media (MSM, in g/L): 0.7 K_2HPO_4, 0.3 KH_2PO_4, 0.01 NH_4SO_4, 0.05 $MgSO_4*H_2O$ supplemented with 0.4 g/L glucose (MSM + G, Sigma-Aldrich) to submerge the plate with the biofilm. The pH was 7.3. The Petri plate was either weighed down to the aquarium bottom by wrapping with a flexible plastic-coated lead flask weight or attaching it using dental glue. Air, pure O_2, or pure N_2 (equating to O_2 concentrations of ~21%, 100%, and 0% by volume in the headspace gas respectively) was introduced through an air stone to maintain gas saturation in the water phase and to provide water movement to ensure good mixing. Concentrations of O_2 in the media assuming saturation of the various gases were calculated from O_2 solubility as a function of temperature, pressure and salinity [12] exchange with the room atmosphere was reduced by using plastic balls (Allplas, Capricorn Chemicals Corp., Secaucus, NY) floating on the water surface.

2.2. Microelectrodes and calibration

O_2 and N_2O microelectrodes with tip diameters of approximately 10–15 μm were fabricated and calibrated as previously described [13, 14].). The dissolved O_2 electrodes were calibrated using a 2 point linear calibration of fully saturated and anoxic sterile media obtained by sparging with pure O_2 and N_2 respectively. For the N_2O electrodes a saturated solution of N_2O was prepared. A dilution series was made to obtain a linear calibration between 0 and 400 μM N_2O. NO microelectrodes with a tip diameter of 15 μm were obtained from Unisense A/S (Aarhus, Denmark). They were calibrated in N_2 flushed water using a NO saturated stock solution to obtain a linear calibration between 0 and 7.3 μM.

The microelectrodes were mounted on micromanipulators positioned opposite of the incubation chamber, connected to a picoampere meters and the signals in picoamperes (pA) were recorded by a data acquisition system (model DAQCard AI16XE50; National Instruments, Austin, TX). Data acquisition and micromanipulator control was performed by laptop using a dedicated program.

2.3. Depth profile measurements and calculations of theoretical nitrate consumption

The microelectrodes were positioned at the surface of the same PAO1 colony using a dissecting scope (Fig. 1). They were positioned at an angle of 45° to the surface, thus the depth was corrected using the Pythagorean theorem. NO profiles were taken in the same colony while sequentially sparging the reservoir water with either air, O_2, or N_2.

2.4. Confirmation of N_2O as a denitrification endpoint in our system

Although PAO1 has the genetic potential to denitrify completely to N_2 [15] *Pseudomonas aeruginosa* has been shown to produce mainly N_2O as an endpoint [16]. We tested whether our biofilms, under the given experimental conditions produce N_2 or N_2O as the primary end product by inhibiting N_2O reductase with acetylene (Yoshinari & Knowles, 1976). The incubation medium was sequentially bubbled with air, N_2 or pure O_2 and alternatingly approximately 20% acetylene was mixed in. During this procedure the biofilm was constantly profiled by an N_2O microsensor. We noted that acetylene addition led to instant swarming and dissolution of the biofilm and to stabilize the biofilm during measurements we coated them with an approximately 50 μm thick layer of

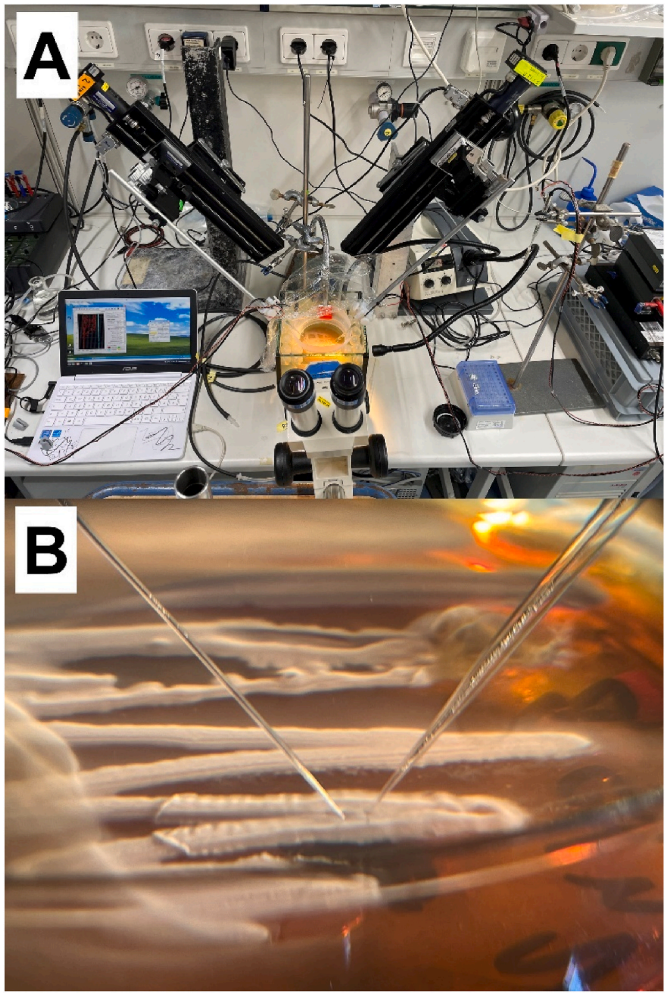

Fig. 1. A) Overview of the experimental set up showing the electrodes entering the reservoir containing the agar plate with the colony biofilm. B) Representative image of dissolved O_2 and N_2O microelectrodes positioned within a *P. aeruginosa* PAO1 colony at as close to the same position as possible. The biofilm colony surface was determined where the tips and shadows of the tips converged and from the signal response.

1% agar, by gently flowing 0.5 ml cooled molten agar (40 °C) over the colonies on the agar plate. Multiple profiles were taken in two independent experiment (Fig. S1) and the maximum flux of N_2O production, which occurred approximately 200 μm depth in the biofilm was calculated from the profiles [13]. Adding acetylene either reduced or did not significantly increase the N_2O production in the biofilms ($P > 0.05$), and also did not change the shape of the N_2O profiles (Fig. 2 and S1). This demonstrated that PAO1 under our experimental conditions performed denitrification to N_2O, and not further to N_2.

2.5. O_2 and NO_3^- flux calculations

The distribution of O_2 and NO_3^- consumption by the colonies at steady state were calculated according to Fick's first law of diffusion: $J = D_c\,(\partial c/\partial x)$, where J is the flux (mol m^{-2} s^{-1}), D_c is the molecular diffusion coefficient (m^2 s^{-1}), and $\partial c/\partial x$, is the local concentration gradient [17]. The N_2O profiles were converted to NO_3^- profiles using

$$(NO_3^-)_x = (NO_3^-)_b - \frac{D_{N2O}}{D_{NO3}} \times (N_2O)_x \times Y$$

with $(NO_3^-)_x$ as the local NO_3^- concentration, $(NO_3^-)_b$ the NO_3^- concentration in the medium, D_{N2O} the diffusion coefficient of N_2O, D_{NO3} the diffusion coefficient of NO_3^-, $(N_2O)_x$ the measured local N_2O concentration, and Y the stoichiometry of NO_3^-/N_2O conversion (mole per mole). Assuming a D_c in water of 2.36×10^{-9} m^2 s^{-1} for O_2, 2.1×10^{9} $m^2 s^{-1}$ for N_2O and 1.84×10^{-9} m^2 s^{-1} for NO_3^- at 24 °C [12,18], and correcting for an estimated reduced effective D_c (D_{eff}) in the biofilm of approximately 58% and 60% respectively [19]. We used a concentration of 1.2 mM NO_3^-, approximating reported concentrations in CF sputum [20]. The local consumption rates of O_2 and NO_3^- were then calculated from the microprofiles as described previously [13]. Subsequently, the local volumetric ATP formation rates were calculated from the local O_2 and NO_3^- reduction rates, with 6.7 ATP/O_2 and 4 ATP/NO_3^-, as reported previously [11].

2.6. Replicates and statistical analysis

We conducted a series of simultaneous measurements on five independent replicate biofilms on separate petri plates over multiple days. In our previous work we noted under air and N_2 at steady state that although profiles were similar for each location they were not the same, likely due to differences in colony size and morphology, local nutrient and mass transfer conditions and activity of the bacteria within the biofilms [8]. A representative additional data set is provided in the supplement.

3. Results

3.1. O_2 flux into the biofilm colony

The O_2 concentrations, controlled by sparging with air, pure O_2 or N_2, varied between 0.04 and 0.9 mM for the first measured biofilm (Fig. 3, S1), corresponding to approximately 23–530 mm Hg. N_2O was developed in the biofilm at all imposed O_2 levels (Fig. 3, S2), although it decreased when the bulk medium was sparged by pure O_2. Immediately upon decreasing the O_2 level in the bulk medium, the N_2O levels, driven by NO_3^- reduction, increased again. Similar results were obtained for replicate experiments (Figs. S2 and S3). We did not detect a threshold concentration of O_2 below which N_2O was produced, rather there was a steady increase in N_2O with a steady decline in O_2.

Examples of O_2 and NO_3^- microprofiles measured inside *P. aeruginosa* agar colony biofilms under different O_2 levels (i.e., O_2 oversaturation, air saturation and O_2 undersaturation), are shown in Fig. 4 and S2. The calculated O_2 and NO_3^- reduction rates and ensuing ATP production show NO_3^- consumption in the oxic and in the anoxic zone. The O_2 penetration depth was controlled by the O_2 concentration in the bulk medium. At the highest imposed O_2 levels, the NO_3^- consumption, and thus the coupled ATP production, decreased in the oxic zone. O_2 penetrated even at elevated medium levels maximally 0.4 mm, leaving a large part of the biofilm anoxic. At an O_2 concentration of ~40 μM O_2, approximately 50 μM NO_3^- was produced. This O_2 concentration is in the range for tissues (~13–90 μM; [21]), and approximately 20% lower than defined hypoxia (<40 mm Hg). This is common for chronic wounds [22]. O_2 penetrated only 0.05 mm, leaving most of the biofilm anoxic.

At decreased O_2 concentrations in the bulk medium, denitrification became proportionally more important, as expected (Fig. 5). During sparging with pure O_2, over 90% of the ATP in the biofilm was produced by O_2 reduction, and when the O_2 level dropped below 60 μM approximately 50% of the energy conservation was driven by NO_3^- reduction.

The NO concentrations in the biofilm varied under different gas conditions (Fig. 6). The highest NO concentrations (~5 μM) were measured under air saturation. Under anoxia the NO concentrations

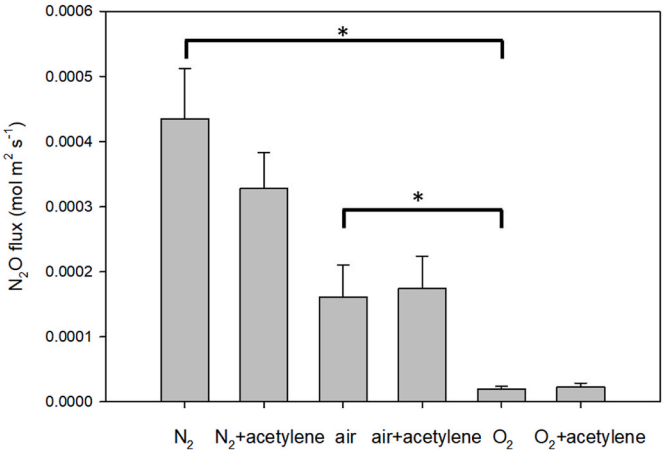

Fig. 2. Maximum N_2O production flux in from multiple profiles of two independent biofilms under different levels of O_2 saturation (N_2, air and O_2) with and without acetylene, a nitrous oxide reductase inhibitor. There was no significant difference between independent replicates or with the addition of acetylene ($P > 0.05$, 2 tailed *t*-test assuming equal variance, d.f. > 8). The flux was significantly decreased under pure O_2 compared to air and N_2 ($P < 0.05$, indicated by *). The surface of the biofilm is at 0 depth. Data are mean and 1 S E., n = 18.13 and 10 for N_2, O_2 and air respectively.

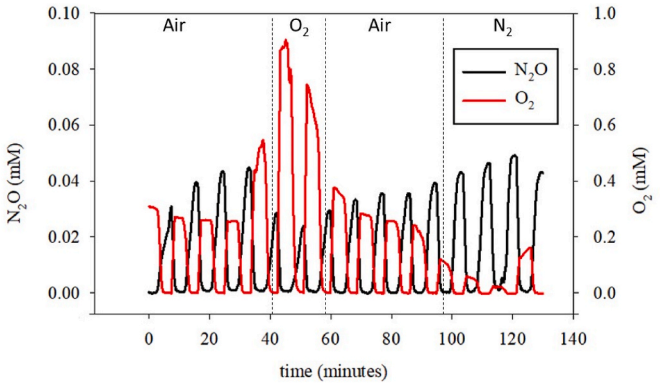

Fig. 3. Time course of the O_2 (red) and N_2O (black) concentrations at approximately the same location within an agar colony biofilm. The first 4 profiles were measured under air saturation, then 3 profiles were recorded while the water column was sparged with pure O_2, followed by 4 profiles under air saturation, and 3 profiles under N_2 sparging. While pure O_2 sparging suppressed N_2O formation, it did not completely stop it. (For interpretation of the references to colour in this figure legend, the reader is referred to the Web version of this article.)

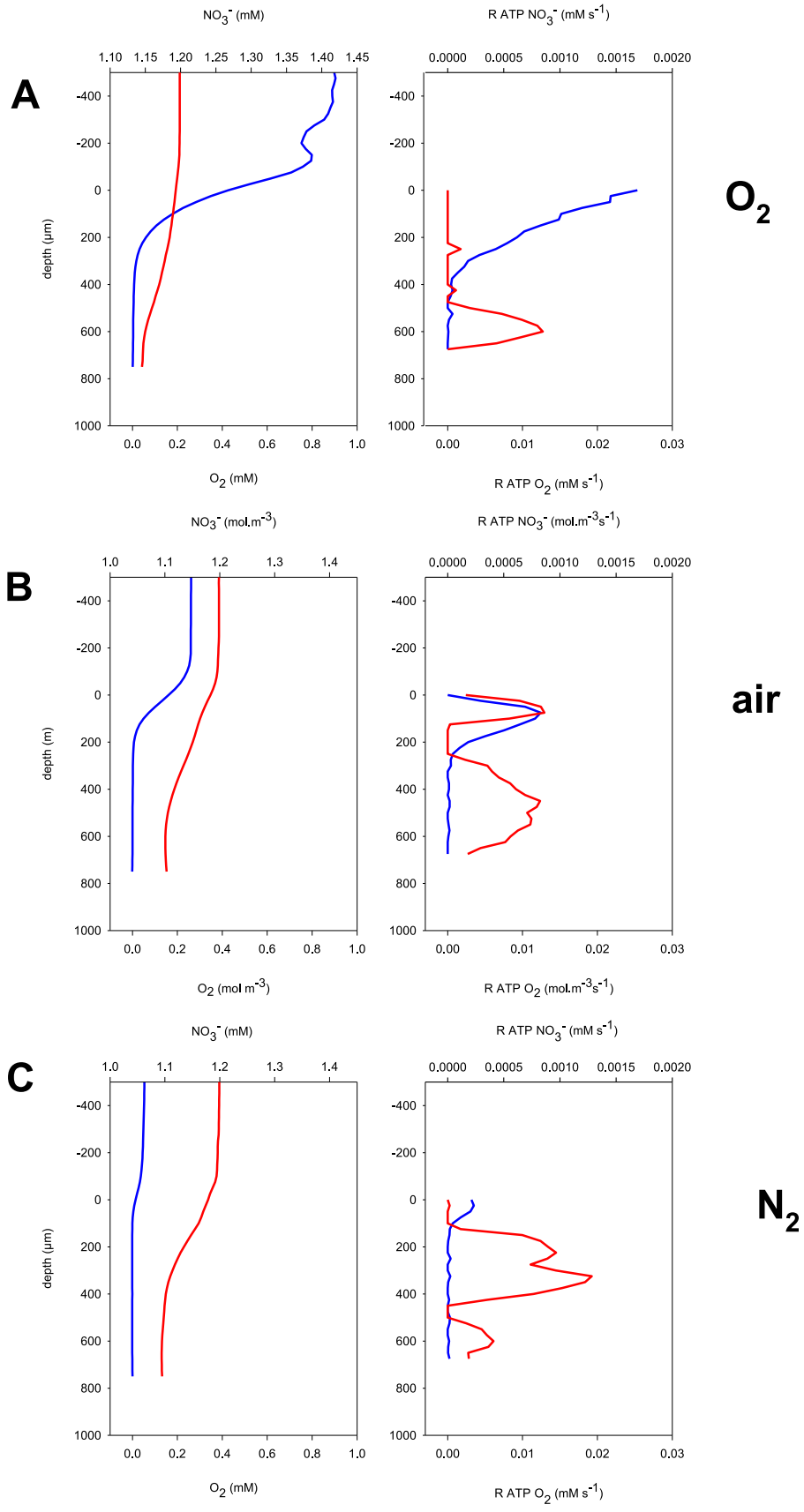

Fig. 4. Representative measured O_2 (blue) and calculated NO_3^- profiles (red) under (a) O_2 oversaturation with sparging pure O_2, (b) air saturation and (c) O_2 undersaturation with sparging pure N_2 (c) in terms of concentration (left panels) and local ATP production rates calculated from O_2 and NO_3^- reduction, respectively (right panels). (For interpretation of the references to colour in this figure legend, the reader is referred to the Web version of this article.)

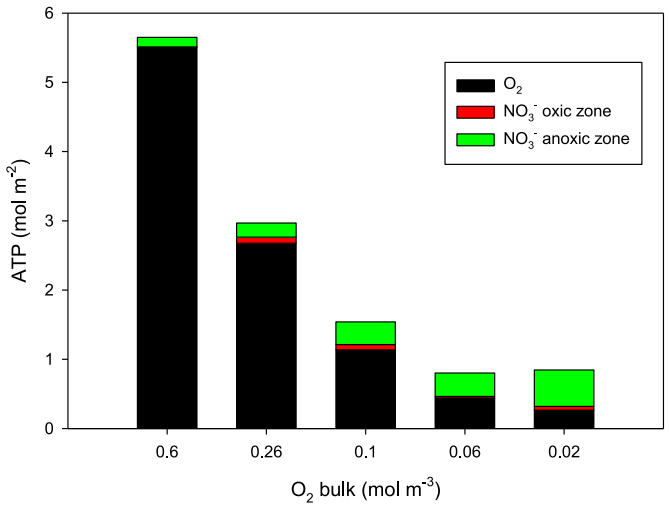

Fig. 5. ATP production rates integrated over the depth of the biofilm, with ATP production by O_2 respiration (black), denitrification in the oxic zone (red), and denitrification in the anoxic zone (green). (For interpretation of the references to colour in this figure legend, the reader is referred to the Web version of this article.)

were lower but still relatively high compared to reported physiological concentrations (~1 μM), and NO almost went to zero under pure O_2 sparging.

4. Discussion

It was recently argued that a detailed description of the microenvironment of living microbial communities is essential for effective treatments of infections [23]. More generally, this holds for understanding the actual behavior of all natural microbial communities. In the present study we used an agar plate colony biofilm model to investigate spatially and temporally resolved O_2 and NO_3^- reduction rates, as well as NO production capability, and inferred energy conservation rates under varying oxygenation conditions. In our biofilms N_2O was the sole product of denitrification and accumulated in the biofilm, despite the strain having the genetic capacity to reduce to N_2 (Fig. 2) [24]. This suggests it is necessary to confirm inferences on physiological processes from genomic information by direct measurements. The accumulation of N_2O during denitrification was shown to occur in *P. aeruginosa* cultures because of inhibition of nitrous oxide reductase by low levels of O_2 (Betlach & Tiedje, 1981) as well as through quorum sensing under high cell densities (Kellermann et al., 2023). However, in our case we saw no effect of acetylene inhibition under anoxic conditions under N_2, ruling this possibility out. The incomplete denitrification with N_2O as the end product allowed us to base NO_3^- fluxes into the biofilm and bioenergetics of denitrification and O_2 respiration on N_2O concentrations and profiles.

The oxic status of the headspace influenced the absolute and relative rates of aerobic respiration and denitrification, and the response to changing headspace gases was relatively rapid occurring at the same location within minutes. When sparged with pure O_2, aerobic respiration was greatly stimulated by a factor of 5; but some denitrification continued. Similar to previous work [8], we found that even under O_2 supersaturation the aerobic respiration rate was so high that anoxic conditions were still produced at the base of the colony, thus allowing denitrification. Since antibiotic susceptibility assays for facultative bacteria, such as *P. aeruginosa* are typically conducted in a humidified 5% CO_2 incubator ($[O_2] \sim 180$ μM) they may not accurately reflect the susceptibility *in vivo* of bacteria if present within a biofilm, as concluded previously [7]. Yet, in the oxic zone, denitrification was suppressed. When the bulk fluid was sparged with pure N_2, denitrification was stimulated due to part of the community switching from aerobic to anaerobic respiration as the conditions became anoxic. The almost instantaneous increase of denitrification upon lowering the O_2 level confirmed that the enzyme system responsible for denitrification was not damaged through oxygenation, but was only temporally inhibited [25]. The bacteria within the biofilm were therefore able to switch their metabolism in response to changing oxic-anoxic conditions rapidly, in the range of seconds to minutes. However, another explanation is that under air and O_2 supersaturation NO, the intermediate precursor to N_2O, is oxidized by O_2 ([26]), and the removal of O_2 contributes to the accumulation of NO and N_2O. Thus under these high O_2 concentration NO_3^- and NO_2^- reduction and the calculated ATP generation from N_2O production may be underestimated.

Biological energy conservation in the form of ATP is not proportional to the thermodynamics of metabolic process, but depends on the number of translocated protons per electron pair shuttled through the electron

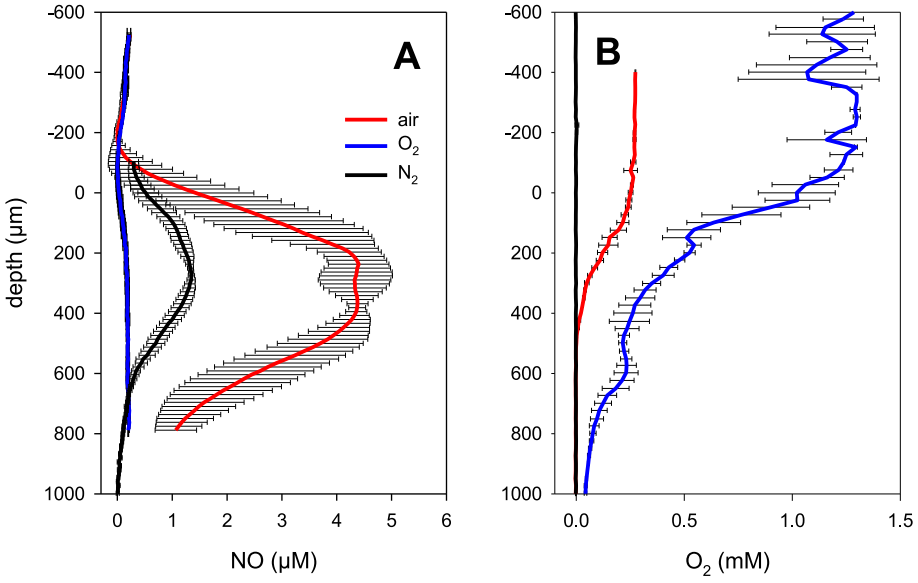

Fig. 6. A) Averaged NO profiles in biofilm incubated under air saturation (red, n = 4), pure O_2 (blue, n = 3) and anoxia under N_2 (black, n = 3) sparged medium over PAO1 cultures, and B) the corresponding O_2 profiles. Mean and 1 standard deviation error bars. (For interpretation of the references to colour in this figure legend, the reader is referred to the Web version of this article.)

transport chains [11]. With O_2 as terminal e-acceptor, 20 protons are translocated per electron pair, while with NO_3^- 12 protons. As the ATP/H^+ stoichiometry is 3 per O_2 respired 6.7 ATP is formed, while per NO_3^- only 4 ATP are formed. Consequently, although O_2 and NO_3^- respiration are thermodynamically close, at equal e-donor supply denitrification will result in lower growth rates than aerobic respiration, as indeed observed [27]. The lower growth rate by denitrification of *P. aeruginosa* PAO1 [5] compared to 1.5/hr (27 min doubling time) from aerobic respiration [27] may lead to reduced susceptibility to antibiotics [28,29]. The doubling time of *P. aeruginosa* biofilm aggregates in CF sputum was estimated to range between 100 and 200 min [27]. In chronic wounds hypoxia (<40 mm Hg O_2) is induced by damage to the vasculature, coagulation and consumption by inflammatory cells [22]. Hypoxia not only limits neutrophil activity against infecting bacteria but also fibroblast and many other host-mediated wound healing mechanisms [22]. Compounding the reduction of local oxygenation due to the inflict of a wound and the presence of bacterial biofilms that compete with host cells for O_2 further depletes the local O_2 concentration. Hyperbaric O_2 is used to correct hypoxia in order to enhance wound healing [30] and has been clinically shown to reduce bacterial load by a small amount [31] and *in vitro* studies show an increased susceptibility to antibiotics, presumably through increasing metabolic activity [32]. However, our data suggests that even if small aggregates of cells are present as seen clinically [33], even under hyperbaric therapy localized regions of hypoxia may occur due to the high rate of respiration, even under O_2 saturation. Biofilms may also induce local regions of hypoxia in the human CF lung as speculated from the expression of *P. aeruginosa* denitrification genes and supporting nitrate concentrations in samples collected from people with CF[5–7]

Denitrification has other implications in the context of biofilm infections. It is documented that denitrification can lead to the accumulation of the physiologically relevant concentrations of NO (120–150 nM) in the anaerobic zones of biofilms [17]. This signaling molecule induces vasodilation, inhibits platelet adhesion, inhibits leukocyte adhesion to endothelia and scavenges the superoxide anions [34,35]. We found unexpectedly high levels of NO, especially at O_2 levels typical for wounds and tissues (20–60 μM). NO levels peaked to 5 μM which is above the threshold for causing mammalian physiological effects [36, 37], and interestingly, over the 1 uM concentration accepted as being toxic to bacteria [38]. Also, under anoxia NO levels were significant, but lower than at low oxygenation. NO was suppressed at high O_2 levels. The NO maximum production we observed at moderate O_2 levels (air sparged) may be explained by the balance between NO production by denitrification (intermediate accumulation enhanced by O_2 as e-transfer to NO_3^- is reduced) and consumption by oxidation (first order to O_2 levels) [26]. Thus at low O_2 concentration NO is low due to efficient reduction to N_2O, at high O_2 concentrations NO is rapidly oxidized chemically, while at intermediate O_2 concentration the production is optimal and degradation minimal. Interestingly, low dose NO is a known mediator of biofilm dispersal [39]. We did observe by eye “clouds”, which we presumed to be a high density of released cells, “billowing” out from the biofilm after a few hours of nitrate addition. *In vivo* this could lead to spreading of an infection. However, the role of NO in both health and disease is complex [40] and the impact of bacterially produced NO in localized infections remains to be elucidated. In future experiments it would be interesting to better correlate this observed phenomenon with NO concentrations within the biofilm.

Our novel approach on making simultaneous measurements at the same micro-location in a single colony allows measuring real-time responses to imposed system perturbations. Due to the technical complexity in setting up such experiments and colony-to-colony variability this technique does not lend itself well to obtain fully optimal replicate data for statistical analysis. However, we believe that our data on the transient response and relative contribution of denitrification and O_2 respiration with respect to spatial distribution and bioenergetics provides insights into metabolic processes possible within facultative aerobic biofilms. Our main conclusion is that metabolic activity within a biofilm colony is strongly influenced by dissolved gases, and that the response in the microenvironment to a change in conditions is rapid. Although under air-saturating conditions the energy yield of aerobic respiration was much higher than that of anaerobic respiration, the relative contribution of energy yield from anaerobic respiration will increase with reducing O_2 levels, as occurs in wounds and infections [22]. Increased mass transfer limitations, e.g. by thicker biofilms or reduced blood supply, will affect O_2 reduction more than NO_3^- reduction, as NO_3^- concentrations are much higher than O_2, and thus its penetration can be much deeper. Denitrification is thus important for energy generation of this pathogen. Secondly, the effect of O_2 on the NO production by these pathogens may well explain the severity of PAO1 infections and understanding this effect will help finding an optimal treatment against infections.

5. Conclusions

1) Although *P. aeruginosa* PAO1 has the genetic potential to denitrify to N_2 in our biofilm system N_2O was allowed to accumulate in the biofilm as the endpoint product, likely due to cell signaling because of high cell density.
2) *P. aeruginosa* PAO1 biofilms can rapidly switch between aerobic oxidation and denitrification in response to changes in O_2 concentrations allowing it to quickly adapt as dissolved gas conditions change.
3) *P. aeruginosa* PAO1 biofilms can rapidly consume O_2, which *in vivo* may afford it the ability to compete with host mediated wound repair and impair the immune response, even under hyperbaric therapy.
4) The expected lower growth rate by denitrifying cells in the oxic and anoxic zones in the biofilm may render these populations less susceptible to antibiotics.
5) At moderate O_2 concentrations as found in tissue and wounds, NO production is the highest and exceeding critical thresholds for physiological effects on host and biofilm, possibly influencing the pathogenicity of *P. aeruginosa.*

FUNDING information

Hanse-Wissenschaftskolleg Institute for Advanced Study (DB and PS). NIH grant R01 R01GM124436 (PS).

Competing interests statement

The authors declare no competing interests.

CRediT authorship contribution statement

Paul Stoodley: Formal analysis, Funding acquisition, Investigation, Methodology, Project administration, Supervision, Writing – original draft, Writing – review & editing. **Nina Toelke:** Investigation, Methodology, Writing – original draft, Writing – review & editing, Formal analysis. **Carsten Schwermer:** Formal analysis, Investigation, Methodology, Writing – original draft, Writing – review & editing. **Dirk de Beer:** Conceptualization, Formal analysis, Funding acquisition, Investigation, Methodology, Project administration, Supervision, Writing – original draft, Writing – review & editing.

Declaration of competing interest

The authors declare that there are no conflicts of interest.

Data availability

Data will be made available on request.

Acknowledgements

We thank Marc Strous (Univ. Calgary) for valuable discussions on bioenergetics, Hans-Curt Flemming (Visiting Professor at the Singapore Center for Life Sciences Engineering,) and Wolfgang Streit (Uni Hamburg) for supplying the PAO1 strain, and all the technicians from the Microsensor Group for preparing excellent microsensors.

Appendix A. Supplementary data

Supplementary data to this article can be found online at https://doi.org/10.1016/j.bioflm.2024.100181.

References

[1] Wu Y-K, Cheng N-C, Cheng C-M. Biofilms in chronic wounds: pathogenesis and diagnosis. Trends Biotechnol 2019;37:505–17.
[2] Tolker-Nielsen T. *Pseudomonas aeruginosa* biofilm infections: from molecular biofilm biology to new treatment possibilities. Apmis 2014;122:1–51.
[3] Stewart PS, Zhang T, Xu R, Pitts B, Walters MC, Roe F, Kikhney J, Moter A. Reaction–diffusion theory explains hypoxia and heterogeneous growth within microbial biofilms associated with chronic infections. NPJ Biofilms and Microbiomes 2016;2:1–8.
[4] Debats IB, Booi D, Deutz NE, Buurman WA, Boeckx WD, van der Hulst RR. Infected chronic wounds show different local and systemic arginine conversion compared with acute wounds. J Surg Res 2006;134:205–14.
[5] Line L, Alhede M, Kolpen M, Kühl M, Ciofu O, Bjarnsholt T, Moser C, Toyofuku M, Nomura N, Høiby N. Physiological levels of nitrate support anoxic growth by denitrification of *Pseudomonas aeruginosa* at growth rates reported in cystic fibrosis lungs and sputum. Front Microbiol 2014;5:554.
[6] Hassett DJ, Sutton MD, Schurr MJ, Herr AB, Caldwell CC, Matu JO. *Pseudomonas aeruginosa* hypoxic or anaerobic biofilm infections within cystic fibrosis airways. Trends Microbiol 2009;17:130–8.
[7] Martin LW, Gray AR, Brockway B, Lamont IL. *Pseudomonas aeruginosa* is oxygen-deprived during infection in cystic fibrosis lungs, reducing the effectiveness of antibiotics. FEMS Microbiol Lett 2023;370:1–8. fnad076.
[8] Schwermer CU, de Beer D, Stoodley P. Nitrate respiration occurs throughout the depth of mucoid and non-mucoid *Pseudomonas aeruginosa* submerged agar colony biofilms including the oxic zone. Sci Rep 2022;12:8557.
[9] Hong WX, Hu MS, Esquivel M, Liang GY, Rennert RC, McArdle A, Paik KJ, Duscher D, Gurtner GC, Lorenz HP. The role of hypoxia-inducible factor in wound healing. Adv Wound Care 2014;3:390–9.
[10] Gao H, Schreiber F, Collins G, Jensen MM, Kostka JE, Lavik G, de Beer D, Zhou HY, Kuypers MMM. Aerobic denitrification in permeable Wadden Sea sediments. Isme Journal 2010;4:417–26.
[11] Chen J, Strous M. Denitrification and aerobic respiration, hybrid electron transport chains and co-evolution. Biochim Biophys Acta Bioenerg 2013;1827:136–44.
[12] Li Y-H, Gregory S. Diffusion of ions in sea water and in deep-sea sediments. Geochem Cosmochim Acta 1974;38:703–14.
[13] Gieseke A, de Beer D. Use of microelectrodes to measure in situ microbial activities in biofilms, sediments, and microbial mats. Molecular microbial ecology manual 2004;2:1581–612.
[14] Andersen K, Kjær T, Revsbech NP. An oxygen insensitive microsensor for nitrous oxide. Sensor Actuator B Chem 2001;81:42–8.
[15] Cui X, Ruan X, Yin J, Wang M, Li N, Shen D. Regulation of las and rhl quorum sensing on aerobic denitrification in *Pseudomonas aeruginosa* PAO1. Curr Microbiol 2021;78:659–67.
[16] Davies KJ, Lloyd D, Boddy L. The effect of oxygen on denitrification in Paracoccus denitrificans and *Pseudomonas aeruginosa*. Microbiology 1989;135:2445–51.
[17] Schreiber F, Stief P, Gieseke A, Heisterkamp IM, Verstraete W, de Beer D, Stoodley P. Denitrification in human dental plaque. BMC Biol 2010;8:1–11.
[18] Versteeg GF, Van Swaaij WP. Solubility and diffusivity of acid gases (carbon dioxide, nitrous oxide) in aqueous alkanolamine solutions. J Chem Eng Data 1988;33:29–34.
[19] Stewart PS. Diffusion in biofilms. J Bacteriol 2003;185:1485–91.
[20] Kolpen M, Kühl M, Bjarnsholt T, Moser C, Hansen CR, Liengaard L, Kharazmi A, Pressler T, Høiby N, Jensen PØ. Nitrous oxide production in sputum from cystic fibrosis patients with chronic *Pseudomonas aeruginosa* lung infection. PLoS One 2014;9:e84353.
[21] Ast T, Mootha VK. Oxygen and mammalian cell culture: are we repeating the experiment of Dr. Ox? Nat Metab 2019;1:858–60.
[22] Hopf HW, Holm J. Hyperoxia and infection. Best Pract Res Clin Anaesthesiol 2008;22:553–69.
[23] Bjarnsholt T, Whiteley M, Rumbaugh KP, Stewart PS, Jensen PØ, Frimodt-Møller N. The importance of understanding the infectious microenvironment. Lancet Infect Dis 2022;22:e88–92.
[24] Vollack K-U, Xie J, Härtig E, Römling U, Zumft WG. Localization of denitrification genes on the chromosomal map of *Pseudomonas aeruginosa*. Microbiology 1998;144:441–8.
[25] Bonin P, Gilewicz M, Bertrand J. Effects of oxygen on each step of denitrification on *Pseudomonas nautica*. Can J Microbiol 1989;35:1061–4.
[26] Lewis RS, Deen WM. Kinetics of the reaction of nitric oxide with oxygen in aqueous solutions. Chem Res Toxicol 1994;7:568–74.
[27] Yang L, Haagensen JA, Jelsbak L, Johansen HK, Sternberg C, Høiby N, Molin S. In situ growth rates and biofilm development of *Pseudomonas aeruginosa* populations in chronic lung infections. Am Soc Microbiol 2008:2767–76.
[28] Nguyen D, Joshi-Datar A, Lepine F, et al. Active starvation responses mediate antibiotic tolerance in biofilms and nutrient-limited bacteria. Science 2011;334:982–6.
[29] Stewart PS, Ghannoum M, Parsek M, Whiteley M, Mukherjee P. Antimicrobial tolerance in biofilms. Microbiol Spectr 2015;3:3. 3.07.
[30] Tejada S, Batle JM, Ferrer MD, Busquets-Cortés C, Monserrat-Mesquida M, Nabavi SM, del Mar Bibiloni M, Pons A, Sureda A. Therapeutic effects of hyperbaric oxygen in the process of wound healing. Curr Pharmaceut Des 2019;25:1682–93.
[31] Sanford NE, Wilkinson JE, Nguyen H, Diaz G, Wolcott R. Efficacy of hyperbaric oxygen therapy in bacterial biofilm eradication. J Wound Care 2018;27:S20–8.
[32] Jensen P, Møller S, Lerche C, Moser C, Bjarnsholt T, Ciofu O, Faurholt-Jepsen D, Høiby N, Kolpen M. Improving antibiotic treatment of bacterial biofilm by hyperbaric oxygen therapy: not just hot air. Biofilm 2019;1:100008.
[33] Thaarup IC, Iversen AKS, Lichtenberg M, Bjarnsholt T, Jakobsen TH. Biofilm Survival strategies in chronic wounds. Microorganisms 2022;10:775.
[34] Moncada S, Radomski MW, Palmer RM. Endothelium-derived relaxing factor: identification as nitric oxide and role in the control of vascular tone and platelet function. Biochem Pharmacol 1988;37:2495–501.
[35] McCall TB, Boughton-Smith NK, Palmer R, Whittle B, Moncada S. Synthesis of nitric oxide from L-arginine by neutrophils. Release and interaction with superoxide anion. Biochem J 1989;261:293.
[36] Cooper CE, Giulivi C. Nitric oxide regulation of mitochondrial oxygen consumption II: molecular mechanism and tissue physiology. American Journal of Physiology-Cell Physiology 2007;292:C1993–2003.
[37] Hall CN, Garthwaite J. What is the real physiological NO concentration in vivo? Nitric Oxide 2009;21:92–103.
[38] Schairer DO, et al. The potential of nitric oxide releasing therapies as antimicrobial agents. Virulence 2012;3(3):271–9.
[39] Barraud N, J Kelso M, A Rice S, Kjelleberg S. Nitric oxide: a key mediator of biofilm dispersal with applications in infectious diseases. Curr Pharmaceut Des 2015;21:31–42.
[40] Lundberg JO, Weitzberg E. Nitric oxide signaling in health and disease. Cell 2022;185:2853–78.